AD/A-006 410

WAVEGUIDE GAS LASERS

Marvin B. Klein

Hughes Research Laboratories

Prepared for:

Air Force Cambridge Research Laboratories

December 1974

DISTRIBUTED BY:

NTIS

National Technical Information Service
U. S. DEPARTMENT OF COMMERCE

UNCLASSIFIED

SECURITY CLASSIFICATION OF THIS PAGE (When Data Entered)

REPORT DOCUMENTATION PAGE		READ INSTRUCTIONS BEFORE COMPLETING FORM
1. REPORT NUMBER AFCRL-TR-75-0005	2. GOVT ACCESSION NO.	3. RECIPIENT'S CATALOG NUMBER AD/A-006410
4. TITLE (and Subtitle) WAVEGUIDE GAS LASERS		5. TYPE OF REPORT & PERIOD COVERED Final Report 1 Dec 1973-30 Nov 1974
		6. PERFORMING ORG. REPORT NUMBER
7. AUTHOR(s) Marvin B. Klein		8. CONTRACT OR GRANT NUMBER(s) F19628-74-C-0096
9. PERFORMING ORGANIZATION NAME AND ADDRESS Hughes Research Laboratories 3011 Malibu Canyon Road Malibu, CA 90265		10. PROGRAM ELEMENT, PROJECT, TASK AREA & WORK UNIT NUMBERS 2001-01-01 62204F
11. CONTROLLING OFFICE NAME AND ADDRESS Air Force Cambridge Research Labs Hanscom AFB. MA 01731 Contract Monitor: Howard Schlossberg/OPL		12. REPORT DATE December 1974
		13. NUMBER OF PAGES 58
14. MONITORING AGENCY NAME & ADDRESS(if different from Controlling Office)		15. SECURITY CLASS. (of this report) Unclassified
		15a. DECLASSIFICATION DOWNGRADING SCHEDULE

16. DISTRIBUTION STATEMENT (of this Report)

Approved for public release; distribution unlimited.

17. DISTRIBUTION STATEMENT (of the abstract entered in Block 20, if different from Report)

18. SUPPLEMENTARY NOTES

19. KEY WORDS (Continue on reverse side if necessary and identify by block number)

Waveguide laser, xenon excimer laser, argon-nitrogen transfer laser, HF electrical laser, capillary discharges

20. ABSTRACT (Continue on reverse side if necessary and identify by block number)

The objectives of this program are to study (both analytically and experimentally) gas laser systems which might operate advantageously in a waveguide configuration. In this analysis phase we examined the scaling of known gas discharge laser systems with diameter. Our interest was in studying performance characteristics which might be improved

DD FORM 1 JAN 73 1473 EDITION OF 1 NOV 65 IS OBSOLETE

UNCLASSIFIED

SECURITY CLASSIFICATION OF THIS PAGE (When Data Entered)

20. (Continued)

in small bore discharges. As a result of this study we were able to identify three systems as being particularly promising: the HF electrical laser, the xenon excimer laser, and the argon-nitrogen transfer laser. These devices had not previously been operated in self-ustained discharges, but we felt they offered considerable promise in discharges in small bore tubes.

In the case of the HF electrical laser, the particular advantage of small bore discharge operation is the control of E/P and the minimizing of discharge nonuniformity and instabilities. We were able to operate pulsed discharges in HF-argon mixtures at conditions which duplicate those used in successful laser experiments using electron beam stabilized discharges. No laser oscillation was observed, probably as a result of contamination of the HF.

Our analysis of the xenon excimer laser and the argon-nitrogen transfer laser indicates that the high specific pump power required could be produced in small bore discharges. Our experiments using 100 μm bore tubes and fill pressures up to 10 atm indicate that power inputs above the calculated threshold level could be produced. Again, no laser action was observed, primarily because of vacuum and mechanical problems which could not be remedied before the end of the program.

PREFACE

The author wishes to thank R. L. Abrams for his helpful guidance and suggestions during this program. G. N. Rupert and A. Standlee provided valuable technical assistance.

TABLE OF CONTENTS

Preceding page blank

LIST OF ILLUSTRATIONS

Preceding page blank

I. INTRODUCTION AND SUMMARY

Since the first report of waveguide laser operation in the He-Ne system,[1] there has been a growing interest in the application of the waveguide concept to other gas laser systems. Unlike conventional resonator lasers, a waveguide laser operates in a smaller diameter discharge region. In this case, optical losses are minimized by making use of the low-loss guided modes which can propagate in the bore, and which couple efficiently to free space modes outside the waveguide. The advantages of operating a gas discharge device in this manner include increased gain per unit length with decreased tube diameter, increased filling factor for the laser mode in the gain region, good discrimination against higher order modes, and a decrease in the physical size of the device.

The most notable application of the waveguide concept has come in the case of the CO_2 system.[2] The optimum pressure in this case increases with decreasing tube diameter, thus producing significant pressure broadening of the gain profile at typical operating pressures. As a result, it has been possible to construct sealed-off CO_2 lasers with a tuning range in excess of 1 GHz.[3] Such a broad tunability is very useful in certain laser communications and radar systems.

Aside from the experiments in CO_2, waveguide laser operation has been demonstrated in two other gas laser systems. Asawa[4] obtained a one watt output at 5% efficiency from a compact sealed-off CO waveguide device. Also, Smith[5] has reported waveguide

Preceding page blank

laser operation in the He-Xe system at 3.5 μm with gains exceeding 1000 db/M.

The objectives of this program are to study other gas laser systems which might operate advantageously in small bore devices. At the beginning of this program, an analytical study of candidate laser systems was performed. As a result of this study we were able to identify two systems as being particularly promising: the xenon excimer laser, and the HF electrical laser. In the first case the specific advantage of capillary bore operation is the ability to produce high pump power densities without excessive gas heating. In the case of the HF system, discharge operation in small bores allows the convenient control of E/P to provide optimum pumping of the laser states. However, at the time of our study neither of these lasers had been operated in a self-sustained electric discharge, so that we were faced with more fundamental problems than the simple scaling of known devices to smaller bores. Because of their promising nature, we decided early in the program to place primary emphasis on these two systems, in spite of the high risk nature of the experiments.

During the second quarter of this program, the first results on the Ar-N_2 transfer laser[6] were published and the program was expanded to include the study of this system. As more results on the system became available, we concluded that it was the most promising for operation in a waveguide capillary discharge. The specific advantages of the Ar-N_2 system are: lower operating pressure and threshold pumping density than the xenon excimer laser, higher gain than the HF electrical laser, and the previously successful operation of the pure nitrogen laser in a self-sustained discharge.

The experimental study of the three systems discussed above proceeded in several stages. In the first two quarters we studied the discharge properties and spontaneous emission spectra of the Xe_2 and Ar-N_2 laser systems in capillary (100 μm diam) discharges. As a result of these studies we developed a design for a metal-ceramic high-pressure discharge vessel which would enable us to attempt waveguide laser action. While this tube was being constructed, we shifted our attention to the HF system. We first studied the discharge properties of HF-rare gas mixtures in order to determine the experimental conditions which produce stable, uniform, sealed-off discharges operating at low values of E/P. As a result of this work, we were able to operate self-sustained discharges in Ar-H_2-HF mixtures which operate at the same values of pressure, voltage, and current as the previously successful experiments performed using electron beam stabilized discharges. However, we were unsuccessful in producing laser oscillation. We believe that there are at least two reasons for this. First, there are indications that HF is lost from the discharge volume by reaction with the tube walls; a slow gas flow would alleviate this problem. Second, the electrically pumped HF laser does not possess high gain, and we were using mirrors of approximately 97% reflectivity. The problem of attaining laser threshold in a new device such as this could be alleviated by operating the device as an amplifier, and probing for gain with a separate oscillator.

In the last quarter of this program the metal-ceramic laser tube was completed, and we returned our attention to the high pressure laser systems studied earlier. Because of the very critical mirror alignment tolerances which result from using submillimeter waveguide diameters, we decided to start with 500 μm diameter tubing (instead of 100 μm), and to operate the discharge first in low pressure argon, in order to align the mirrors using the high gain laser transition at 4880 Å. Unfortunately, unexpected vacuum, alignment and discharge problems slowed this work down considerably. At the end of the contract period, we had obtained laser action at the argon 4880 Å wavelength, but we did not have sufficient time to study the $Ar-N_2$ or the Xe_2 systems. We feel that there are several factors which might prevent the achievement of discharge-excited waveguide laser action in the Xe_2 system, but that there is a high probability of success in the case of the $Ar-N_2$ system.

This report is organized in four sections. Section II describes briefly the scaling of several gas discharge laser systems to smaller bores. In Section III we discuss our experiments on the HF electrical laser, and in Section IV our analysis and experiments on the xenon excimer and $Ar-N_2$ transfer laser are presented.

II. SCALING OF GAS LASERS

In this section we will briefly examine the scaling of discharge pumped gas laser systems in small bores. The goal is to identify some performance characteristic (e.g., threshold pump power, output power, linewidth) which is significantly improved in small bore tubes. The systems which were reviewed include He-Ne, He-Xe, He-Cd, argon and other ion lasers, and atomic copper vapor. Much of the discussion presented here is based on a general review of discharge similarity rules by Francis[7] and discussions of scaling in He-Ne lasers[8] and CO_2 lasers.[9]

In studying the properties of laser discharges in varying bore sizes, we seek a common basis for comparison. It has been shown[7] that the most useful criterion is that the electron temperature and gas temperature must remain constant. The performance of most gas lasers is a sensitive function of electron temperature, so that by holding this parameter fixed we can judge the effects of other factors on laser parameters. For a given gas fill the electron temperature is a unique function of the parameter PD, where P is the pressure and D is the bore diameter. Thus, fixing the electron temperature implies the condition PD = constant. It is not surprising that most gas lasers scale with diameter so that gain is optimized at constant PD. The magnitude of the optimum gain does not necessarily remain constant as the tube diameter changes (at constant PD), and in fact, for the gas laser systems of interest here, the gain increases with decreasing diameter; the exact variation lies in the range D^{-1} to D^{-2}. The increase of gain in small bore tubes allows a reduction in tube length required for reaching threshold, but has no fundamental advantage from an overall performance point of view.

A more important parameter describing the performance of a gas laser system is the available output laser power per unit length. In many systems the laser power per unit volume increases in small bore tubes, but in all cases considered the power per unit length remains constant or even decreases. This is an important result, and it suggests that other performance factors which scale advantageously must be found before continuing studies of a given gas discharge system in a small bore tube.

In the CO_2 system a significant performance factor is the output linewidth. As mentioned in Section I, the CO_2 laser gain profile is significantly broadened at the high pressures which are characteristic of small bore operation. The resulting large bandwidth is of considerable practical importance. Among the other gas laser systems included in our review of scaling, none possesses the similar line broadening advantage, mostly because the intrinsic doppler width is much larger ($\simeq$ 1 GHz) than in CO_2 ($\simeq$ 50 MHz).

Among the other characteristics of interest are the thermal properties and cooling capability of small bore discharges. If we require a constant gas temperature on axis, then the input power per unit length is invariant with tube diameter, so that there is no thermal advantage of operating in small bore tubes.

A more thorough discussion of the thermal properties of capillary discharges is given in Section IV.

In the pulsed atomic copper vapor laser, a performance characteristic of particular importance is the maximum repetition rate permissible before degradation of the laser peak power occurs. This rate is determined by the lifetime of atoms in the lower laser level, which is metastable. It is easy to show that regardless of whether metastable destruction occurs by volume collisions with electrons or by diffusion to the walls, the limiting repetition rate increases in small bore tubes. This is a significant advantage in obtaining higher average power. However, the copper laser is a very high gain device, especially if operated in a small bore tube. Thus particular attention would have to be paid to the control of gain in a waveguide resonator in order to avoid parasitic superradiance. Furthermore, the technological problems of designing and building an experimental copper vapor laser are considerable.

As a result of our scaling analysis of the more common gas laser systems, we concluded that (other than CO_2 and CO) none offered clear advantages in a small bore waveguide geometry. We then proceeded to consider several other gas laser systems which are not subject to the usual scaling laws, but which have promising application in small bore discharges. These are discussed in the following sections.

III. HF ELECTRICAL LASER

A. Introduction

The HF or DF chemical laser has proved to be a very useful device for producing high cw power at good efficiency in the 2.5 to 4 μm region.[10] In particular, the wavelengths for DF operation (3.5 to 4 μm) lie in a spectral region of low atmospheric absorption and are thus attractive for communications and radar applications. However, the cw HF (or DF) chemical laser suffers from several practical disadvantages: it requires a steady flow of substantial amounts of F_2 (or SF_6) and H_2 (with accompanying flow hardware and vacuum pump), it cannot be readily scaled down to lower powers, and it does not always possess adequate medium homogeneity.

As a result of the above factors there has been considerable interest in exciting the laser transitions in HF (or DF) by direct electrical pumping, in an analogous manner to lasers using CO_2 and CO. The advantages of electrical pumping of HF include: low fuel requirements (with the possibility of sealed-off operation), high efficiency, small size, and improved frequency stability resulting from better homogeneity of the active medium.

Recent published work[11] has reported the successful electrical pumping of HF (or DF) using an electron beam stabilized discharge. Laser action was observed on several vibrational-rotational lines in HF-Ar (or DF-Ar) mixtures containing less than 1% HF (or DF), with total pressures on the order of 200 Torr. Typical values of E/P were in the range 0.4 to 1.8 V/cm-Torr, while the peak current density was typically 4 to 10 A/cm^2.

The small partial pressures ($\simeq$ 1 Torr) of the HF or DF are required to avoid discharge instabilities and to reduce V-T relaxation, which would destroy the partial inversion. These experiments have demonstrated that direct electron impact excitation of vibrational states in HF or DF is effective in producing a partial inversion in these materials at room temperature. The authors of these studies also observed enhancement of the output of certain lines in HF due to excitation transfer from vibrational states in H_2, which was present as a discharge additive. Similar results were also obtained in D_2-DF mixtures.

The principal advantages of using electron beam stabilization in the above experiments are discharge uniformity resulting from uniform volume ionization by the electron beam, and independent control of E/P due to the existence of an external sustaining source. The control of E/P is essential, because low values of E/P (which is proportional to electron temperature) are required to prevent dissociation of the HF by electron collisions. Recent kinetic modeling calculations on HF-rare gas discharges[12] have shown that the threshold value of E/P for significant collisional dissociation is approximately 4 V/cm-Torr.

In a self-sustained cw glow discharge, E/P is invariant for fixed values of pressure and bore radius (except for a weak dependence on current). However, as mentioned earlier the electrical HF laser appears to optimize at buffer gas pressures near 200 Torr. Since the quantity E/P decreases with pressure, it was felt that sufficiently low values of E/P might be obtainable in a self-sustained glow discharge at these pressures, especially using buffer gases of low ionization potential. Since cw high pressure glow discharges can suffer from instabilities and spatial nonuniformity, it was felt that operation in small bores was desirable to minimize these effects. The need for small bore operation suggests the use of a waveguide resonator in order to reduce laser cavity losses. In particular, for a 10 cm long laser bore and a wavelength of 2.5 μm, optical diffraction losses using a conventional confocal resonator become appreciable for bore diameters less than 1 millimeter (where the Fresnel number is unity).

B. Experiments

In order to investigate the discharge and laser properties of HF-rare gas glow discharges, we constructed the tube shown in Fig. 1. The tube was constructed of Pyrex, with CaF_2 Brewster windows and an integral water jacket for cooling. The vacuum and gas fill system used in these experiments was specially constructed to withstand HF attack. Stainless steel construction was used wherever possible, although for convenience some components (e.g.,the discharge tube) were constructed of glass. At the low HF partial pressures involved in our experiments ($\simeq$ 1 Torr), it was felt that corrosive attack by HF would be within acceptable limits. The HF purchased for these experiments was quoted at 99.9% purity. Since impurities such as water vapor can produce significant vibrational thermalization in HF, the purchased HF was purified by distillation and transferred in small quantities (several grams) into a sample cylinder for use

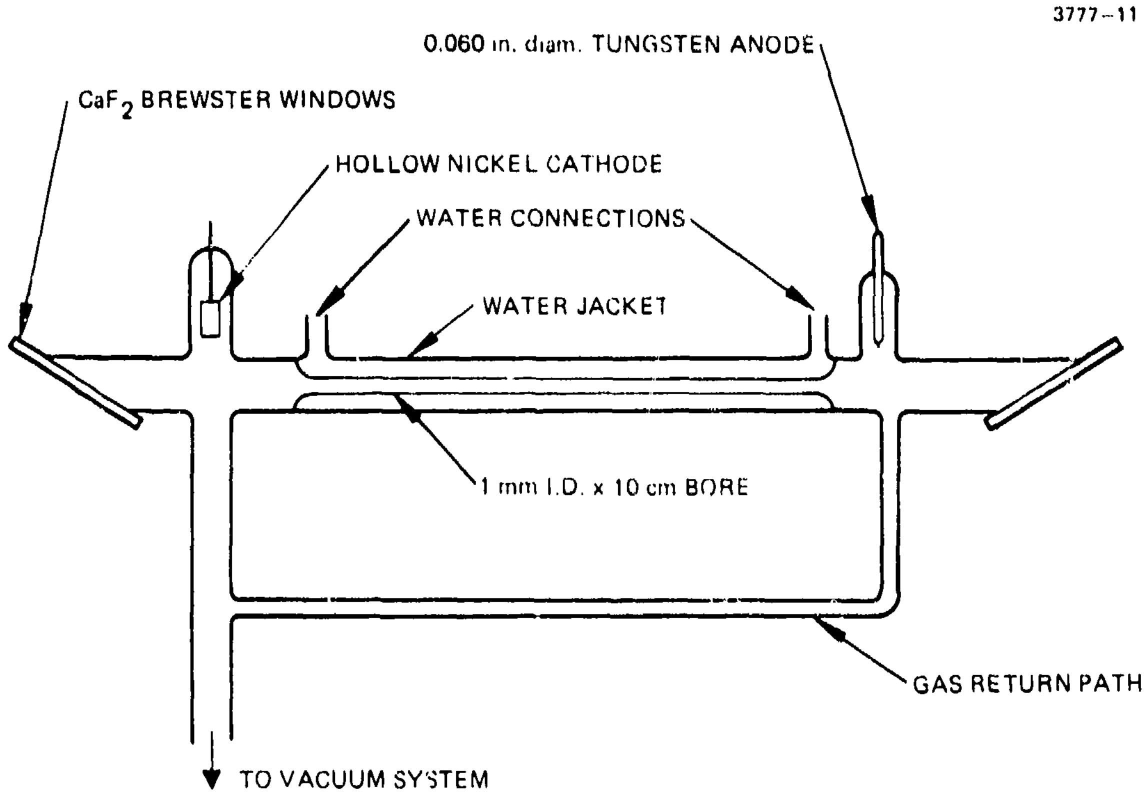

Fig. 1. HF discnarge tube construction.

in our experiments. The vacuum system contained a large stainless steel mixing chamber, where discharge mixtures were measured and allowed to equilibrate for several minutes before being admitted to the discharge tube. All other gases used were of research grade purity.

The first stage of our experimental study was to determine the optimum buffer gas constituent for use in our laser experiments. Our choice was limited to the rare gases, since they provide lower values of E/P and lower values of HF vibrational relaxation cross section than other gases. Four criteria were used to determine the relative effectiveness of each rare gas tested (helium, argon, and xenon): E/P values, radial uniformity of the discharge, stability of the discharge current and voltage, and the degree of dissociation in mixtures with HF or H_2. Each criterion is considered separately below. All measurements were performed at a dc discharge current of 3.5 mA, using a 1.6 MΩ ballast resistor.

Variation of E/P. In rare gas discharges at constant pressure, E/P decreases with atomic number of the species, since the ionization and excitation potentials are decreasing. This same variation is observed when small fixed amounts of HF or H_2 are added to the discharge. Quantitative results will be discussed later.

Radial Uniformity. The threshold pressure for visible contraction of the discharge column was approximately 50 Torr in xenon, 250 Torr in argon, and greater than 300 Torr in helium.

The addition of small amounts of HF or H_2 did not significantly affect these values. The tendency to contraction in the heavier rare gases is thought to be due to their low values of thermal conductivity and ambipolar diffusion coefficient.

Discharge Stability. For certain discharge conditions, strong coherent oscillations ($\nu \simeq 50$ kHz) appeared on both the current and voltage waveforms. These oscillations were frequently accompanied by flickering on the outside of the cathode, instead of a uniform, stable discharge inside it. However, dimensional adjustments and modification of the cathode to include an insulating coating on the outside did not significantly improve discharge stability. In general, the lighter rare gases yield more stable discharges at a given pressure than the heavier rare gases.

Dissociation of HF and H_2. For a given rare gas-HF (or DF) mixture, dissociation of the molecular constituent increases with E/P. However, in evaluating the relative dissociation effects of the various rare gases, other mechanisms besides electron collisional dissociation may be present. These might include dissociation by collisions with excited rare gas atoms, or penning ionization combined with dissociative recombination in the molecule. In order to measure the relative amount of dissociation produced by each rare gas, we have measured the sidelight intensity of the 4862 Å balmer line in atomic hydrogen (H_β) for HF-helium and HF-argon mixtures at total pressures between 35 and 200 Torr. Our measurements were taken several minutes after discharge ignition at which time the H_β intensity had stabilized to a value typically

20% larger than its initial value. The results are plotted in Fig. 2. We see that at a given pressure helium produces nearly two orders of magnitude more H_β intensity than argon, and thus approximately 100 times more dissociation. Although the effects of xenon were not studied in detail because of the early onset of discharge contraction, the H_β intensities in low pressure HF-xenon mixtures were more than 10 times lower than those from the HF-argon mixtures. We also note that the H_β intensities decrease with pressure for a given buffer gas (as expected), due to the accompanying decrease in E/P.

To review the above discussion, the criteria of low E/P and low dissociation favor the use of the heavier rare gases, while the criteria of radial uniformity and discharge stability favor the lighter rare gases. The best compromise between these conflicting requirements is the use of argon. We are able to operate stable, uniform discharges in 0.5% HF-Ar mixtures at pressures up to 200 Torr. The lowest measured value of E/P (2.1 V/cm-Torr) occurred at 200 Torr. This compares with a measured value of 0.6 V/cm-Torr in pure argon at the same total pressure.

From the above measurements we see that E/P values somewhat below those expected to produce significant dissociation are attainable in self-sustained cw discharges in 0.5% HF-Ar mixtures. On the basis of this observation we set about to search for laser action in this mixture, using two silver coated mirrors in a conventional resonator design. A conventional resonator was chosen because our particular type dimensions could support a TEM_{00} mode. The resonator was aligned by operating the same discharge

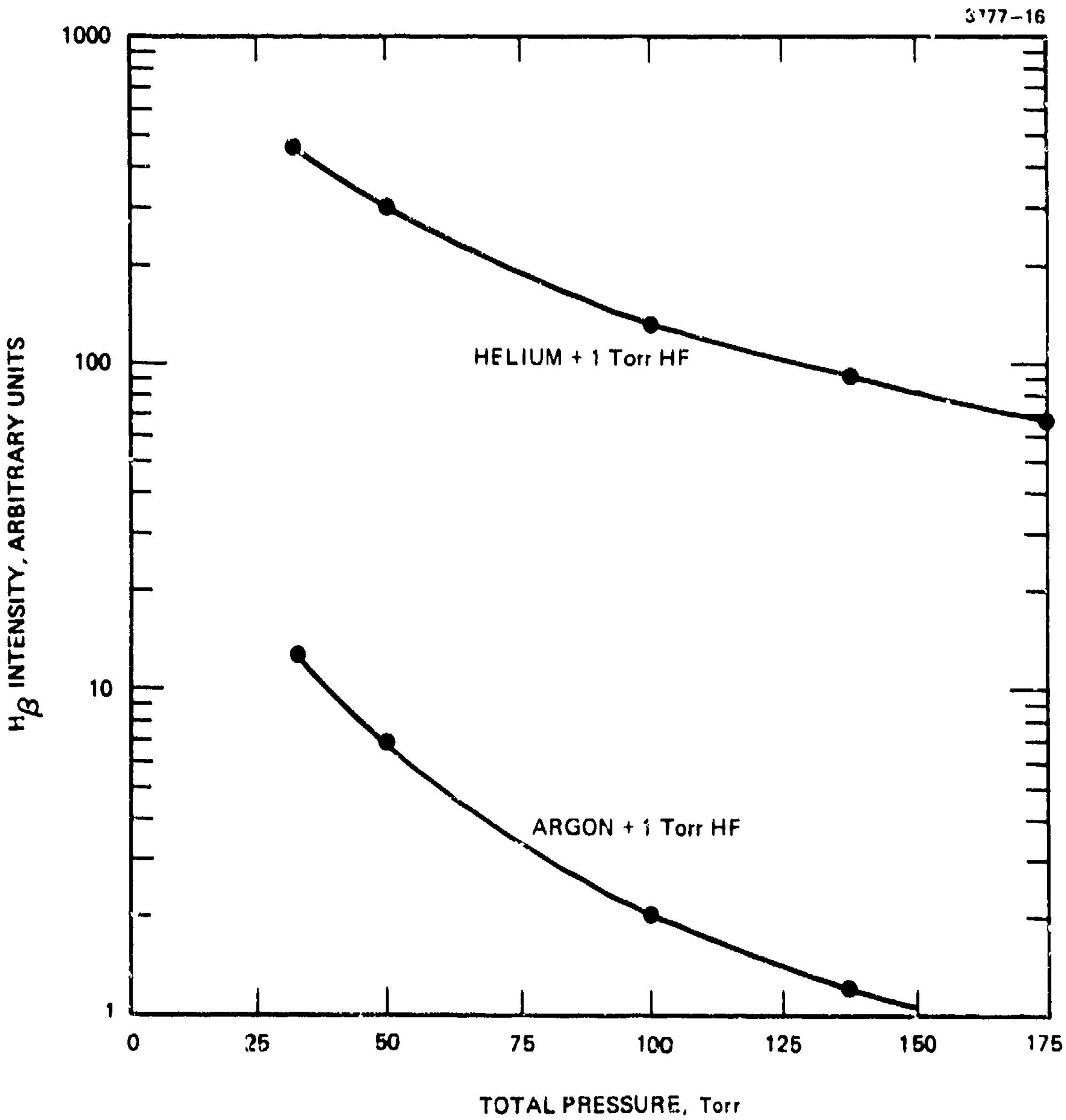

Fig. 2. H_β intensity versus total pressure for HF-helium and HF-argon mixtures.

tube with a He-Ne fill, and optimizing the output at 3.39 μm. The detector used was a liquid nitrogen cooled InSe photovoltaic device aligned to receive radiation reflected from a Brewster angle window. We examined discharges in mixtures containing 0.5 to 1% HF at total pressures in the range 50 to 200 Torr, as well as varying amounts of hydrogen additive in the range 0 to 10%. The discharge current was varied from 3 to 30 mA, corresponding to current densities in the range 0.4 to 4 A/cm^2. No laser oscillation was observed for the range of experimental parameters given above. There are several possible explanations for these negative results: the large steady-state specific power input at the higher current levels ($\simeq 10^3$ W/cm^3) might have produced excessive thermalization of the vibrational states, or the HF in the gas fill might have been removed from the discharge volume by slow dissociation or reaction with the tube walls.

Although the loss of HF in the above experiment can be compensated by gas flow, the large power dissipation (and gas heating) at the reported threshold current density and the relatively high values of E/P sustained over long periods of time are more difficult to overcome, and reduce the chances for attaining laser threshold in an experimental device such as ours. A more reasonable way to optimize the laser properties of our discharge would be to measure gain with a probe laser, and then adjust the various discharge parameters for optimum. Since an HF probe laser was not available, we decided to turn our attention to pulsed discharges, where gas heating is reduced, and which afford the opportunity for better control of E/P.

In considering techniques for pulsing the HF discharge, we felt it was essential to develop a scheme which permits operation at lower values of E/P than were attainable in the cw experiments. For this reason, a standard capacitor storage discharge using thyratron switching was considered to be unsatisfactory. Instead we decided to investigate techniques for operating pulsed discharges in our standard tube design which are not self-sustained, and which operate at controllable v lues of E/P. One possible technique for achieving this goal is to preionize the discharge by some means, and then use an applied dc voltage (below the sustaining level) to induce electron collisions and laser pumping. Although this type of discharge is externally sustained in the sense that an initial distribution of electrons is produced independently, the remaining portion of the discharge is not externally or self sustained, and thus it terminates in a time characteristic of the acting electron loss mechanisms. Generally, these times are sufficiently long ($\simeq$ 100 μsec in our tube) at higher pressures to allow meaningful study of potential laser characteristics.

One technique for implementing the above scheme has been developed previously for the study of CO_2 waveguide TEA lasers.[13] In this technique the initial ionization is provided by a short-pulse (low energy) capacitor discharge, while a constant dc voltage (below breakdown) is used to produce an afterglow at low E/P. This technique has been very successful in producing discharge conditions which closely duplicate optimum conditions in externally sustained CO_2 TEA lasers. On the basis of these results, we set about to apply this same technique to the HF-argon mixtures studied earlier. A schematic diagram of our discharge circuit is shown in Fig. 3. The value of the ballast resistor R was variable between 100 and 100 kΩ; its purpose was to limit the discharge current in case of dc breakdown, and to provide for convenient adjustment of the afterglow current. A typical current and voltage pulse (in a 1% HF-Ar mixture at 100 Torr) taken from an oscilloscope trace is shown in Fig. 4. Similar results are obtained at 50 and 100 Torr. Using Fig. 4 as a reference we can make several observations regarding the performance of this discharge circuit.

1. A significant portion of the discharge energy appears in the large initial current pulse. At the lowest values of thyratron voltage which provide stable triggering, the peak current is greater than one ampere. The introduction of a current-limiting resistor in the thyratron circuit leads to irregular triggering. Variation of the discharge capacitance C had little effect on the pulse width or peak current.

2. The discharge voltage at the time of peak current is equal to the preset dc value V_1.

3. There is a substantial afterglow, leading to tails on both pulses which are approximately 100 μsec in duration. The current amplitude during this portion of the pulse could be readily varied between 50 mA and 2 A by varying the ballast resistance R. The voltage during the afterglow was on the order of 100 V.

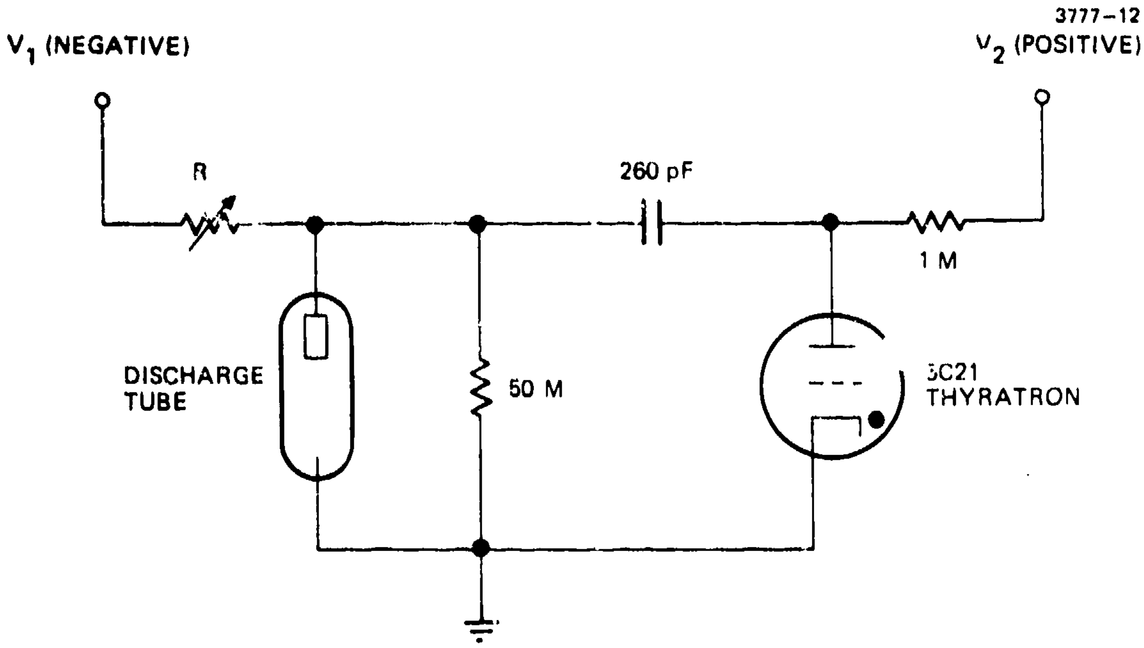

Fig. 3. Preionized pulsed discharge circuit.

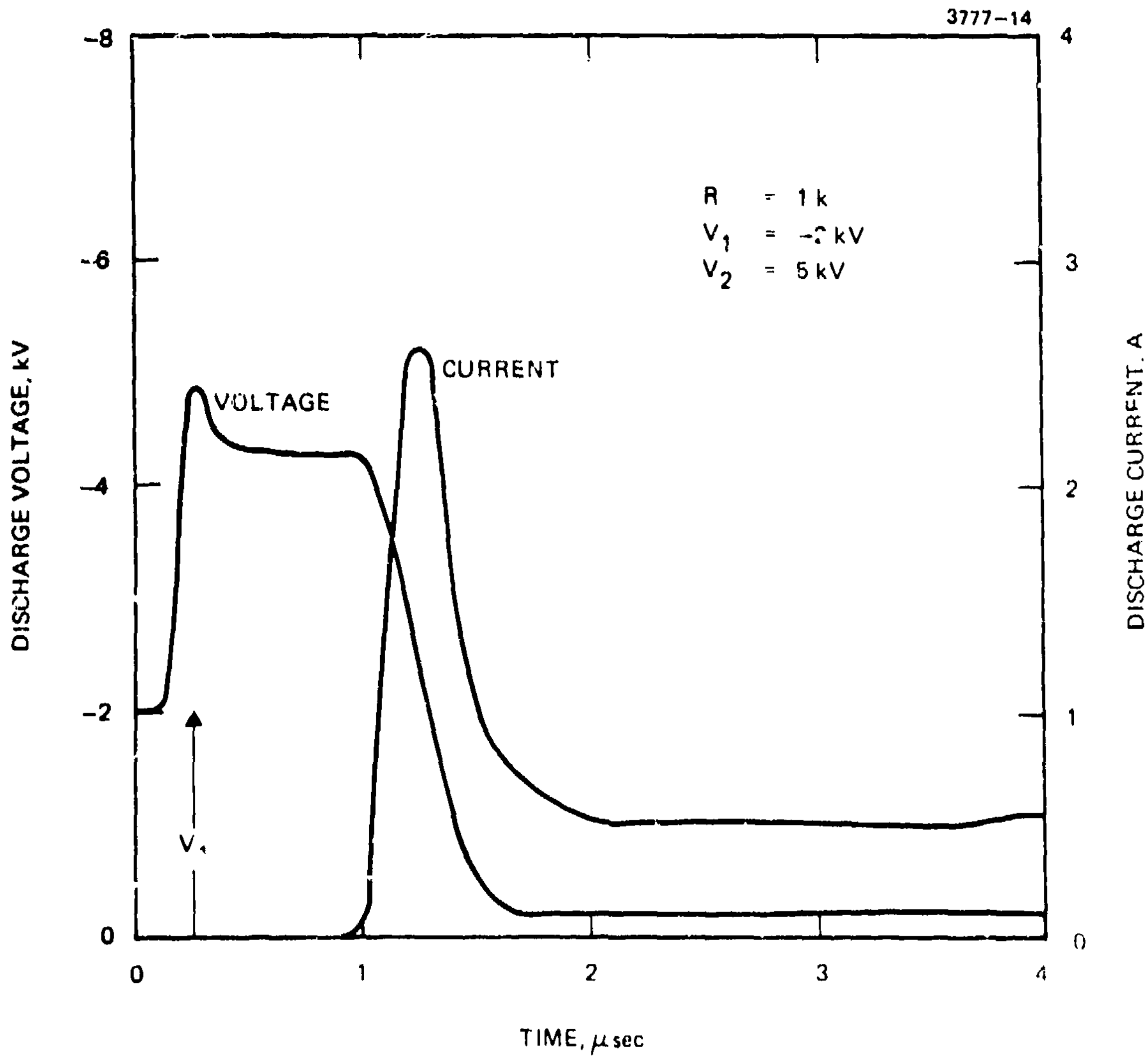

Fig. 4. Voltage and current waveforms for capacitor triggered discharge.

On the basis of the above measurements we concluded that this scheme of discharge pulsing is not optimum for pumping the HF laser transitions. It is felt that too much energy is deposited into the discharge during the first pulse, leading to heating and dissociation which prevent making use of the very low E/P conditions during the afterglow. Nevertheless, we did make an attempt to produce laser oscillation with this discharge scheme using the same gas mixtures tried earlier and varying levels of afterglow current; however, no laser output was observed.

In considering possible refinements of our laser discharge pumping technique, we felt that it was important to be able to preionize the discharge without depositing large amounts of energy into the gas. In order to accomplish this we decided to try removing the capacitor discharge portion of our circuit and instead try using a voltage rf pulse applied to an external trigger wire (wrapped around the tube) to preionize the discharge. Typical peak-to-peak values of pulse voltage were $\simeq$ 40 to 50 kV. This pulsing technique deposits very little power into the discharge, but it also does not produce the level of ionization which the capacitor discharge could provide. When this trigger pulse was applied to our discharge with dc voltages present at the electrodes, we observed that there was a narrow range of dc voltages (just below the dc breakdown voltage) which induced a long discharge pulse which delayed spontaneously. At higher settings of dc voltage, spontaneous discharge breakdown occurred, and at lower values no discharge at all was observed. A typical current and voltage trace during triggered discharge operation (of a 1% HF-Ar discharge at 100 Torr) is shown in Fig. 5. The peak current was readily adjustable between 50 mA and 500 mA by varying the ballast resistance R. On the other hand, the discharge voltage remained relatively constant near 500 V for this range of currents. This invariance of discharge voltage, and the operation of this device just below dc breakdown suggests that this discharge is partially self-sustaining. However, it is still very attractive for electrical pumping of HF, since the voltage (and thus E/P) is low, and the current is readily adjustable. In particular, our measured values of E/P and current density at both 100 and 200 Torr fall within the range of values found in Ref. 11 to be optimum for electrical pumping of HF in an electron beam stabilized discharge. Significantly, we have duplicated these conditions in a much more compact device.

On the basis of these successful pulsed discharge experiments we again aligned our laser cavity using the He-Ne 3.39 μm transition, and searched for laser action in HF-Ar mixtures in the pressure range 50 to 200 Torr; again we were unsuccessful. We still feel that this discharge technique is most promising for the excitation of the HF laser transitions, and feel that several experimental adjustments could be made to improve the likelihood of success. First, as mentioned before, the use of a probe laser to measure gain would be very helpful for optimization purposes. Secondly, improved mirror coatings (using dielectric materials) would significantly reduce cavity losses when a resonator is used. Third, the use of flowing gas would remove the possibility of cleanup or contamination which exists in sealed-off discharges. Finally, further purification of the purchased HF might aid in reducing contamination. We hope to effect these improvements in later work

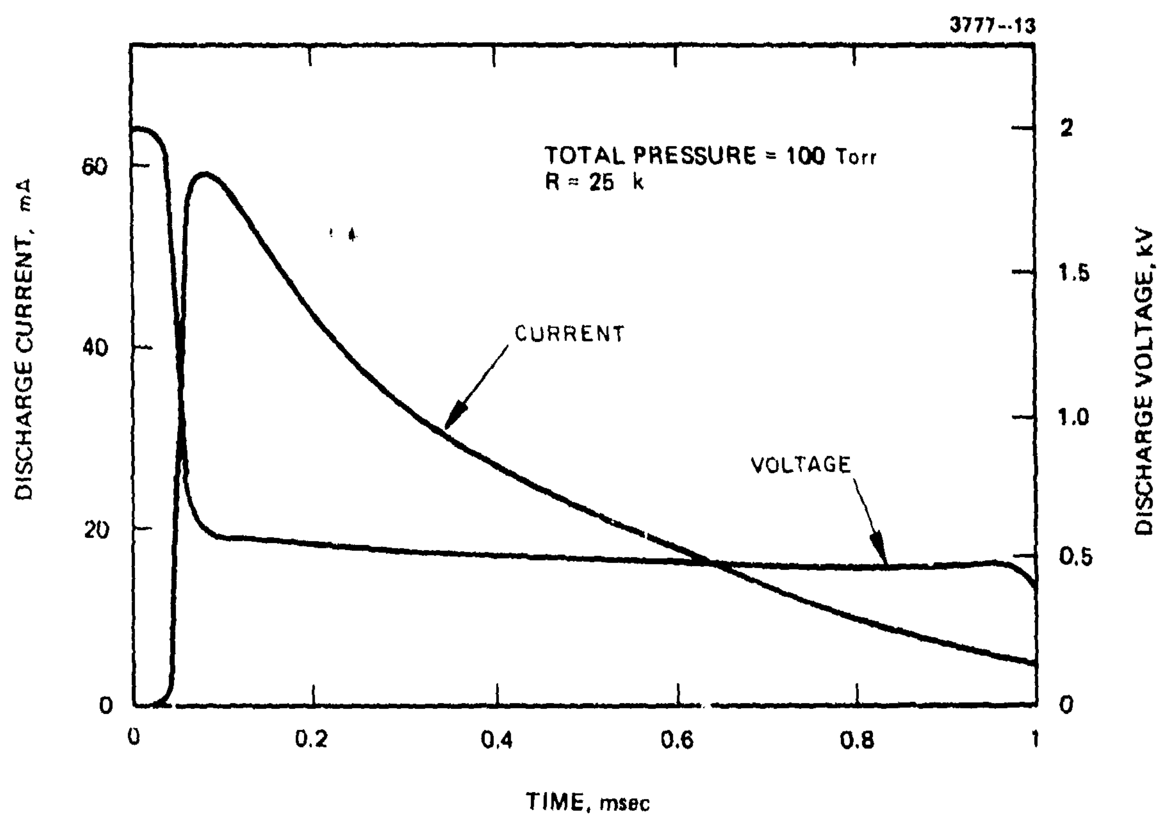

Fig. 5. Voltage and current waveforms for an rf triggered discharge in a 1% HF-Ar discharge.

IV. XENON EXCIMER AND ARGON-NITROGEN SYSTEMS

A. Introduction

Since the first report of laser action near 1730 Å in high pressure xenon,[14] there has been considerable interest in high pressure gas lasers as potential high energy, efficient sources in the 1000 to 2000 Å region. For similar reasons, the recent report of laser action at 3571 Å in high pressure argon nitrogen mixtures[6] has stimulated interest in this system. However, both systems in the past have suffered from a significant drawback in operating convenience: they have been operated only with electron beam pumping, which adds considerable experimental complexity to the basic discharge tube design. The principal reason for using electron beam pumping is that it allows the uniform deposition of high specific energies into large gas volumes at high pressures. The pumping of these systems by self-sustained gas discharges was not attempted, presumably because such discharges are highly constricted and nonuniform at high pressures and produce considerable local heating. We believe that all these drawbacks can be overcome by operating in discharge tubes whose diameter is comparable in size to the diameter of the constricted discharge (typically 50 to 200 μm in xenon above one atmosphere). In such a case the discharge should be stabilized by the tube walls and is expected to be uniform over its cross section. Also, the close proximity of the walls to the discharge acts to provide significant conductive cooling of the gas. This latter factor is especially significant in the xenon excimer system, since the laser could be made to operate in a cw mode if adequate cooling can be provided.

Once the requirement of submillimeter bore diameter is established, it is most convenient to consider a waveguide resonator for such a system. For capillary bore tubes of any significant length the diffraction losses of free space modes inside the laser tube would be prohibitively high. On the other hand, the waveguide concept makes use of the low loss guided modes which can propagate in the laser bore and which can couple efficiently to free space modes outside the bore.

B. Review of Excitation Mechanisms

1. Xenon Excimer Laser

Laser action in electrically excited high pressure xenon arises from transitions in the Xe_2 molecule. This molecule (along with those of the other rare gases) is only weakly bound (by Van der Waals forces) in its ground state, while it possesses numerous stable excited electronic states; such a molecule is known as an excimer. A simplified energy level diagram of the Xe_2 molecule is given in Fig. 6. The laser transition at 1730 Å in Xe_2 originates from the lowest excited electronic states ($^1\Sigma_u^+$ and $^3\Sigma_u^+$) and terminates on the repulsive ground state ($^1\Sigma_g^+$). Since the ground state is unstable, it is weakly populated and thus presents no bottleneck to pulsed or cw operation; in fact, nearly 100% population inversions should be possible.

The electrical excitation of the laser transition in Xe_2 is thought to proceed through a series of interactions summarized below[15]:

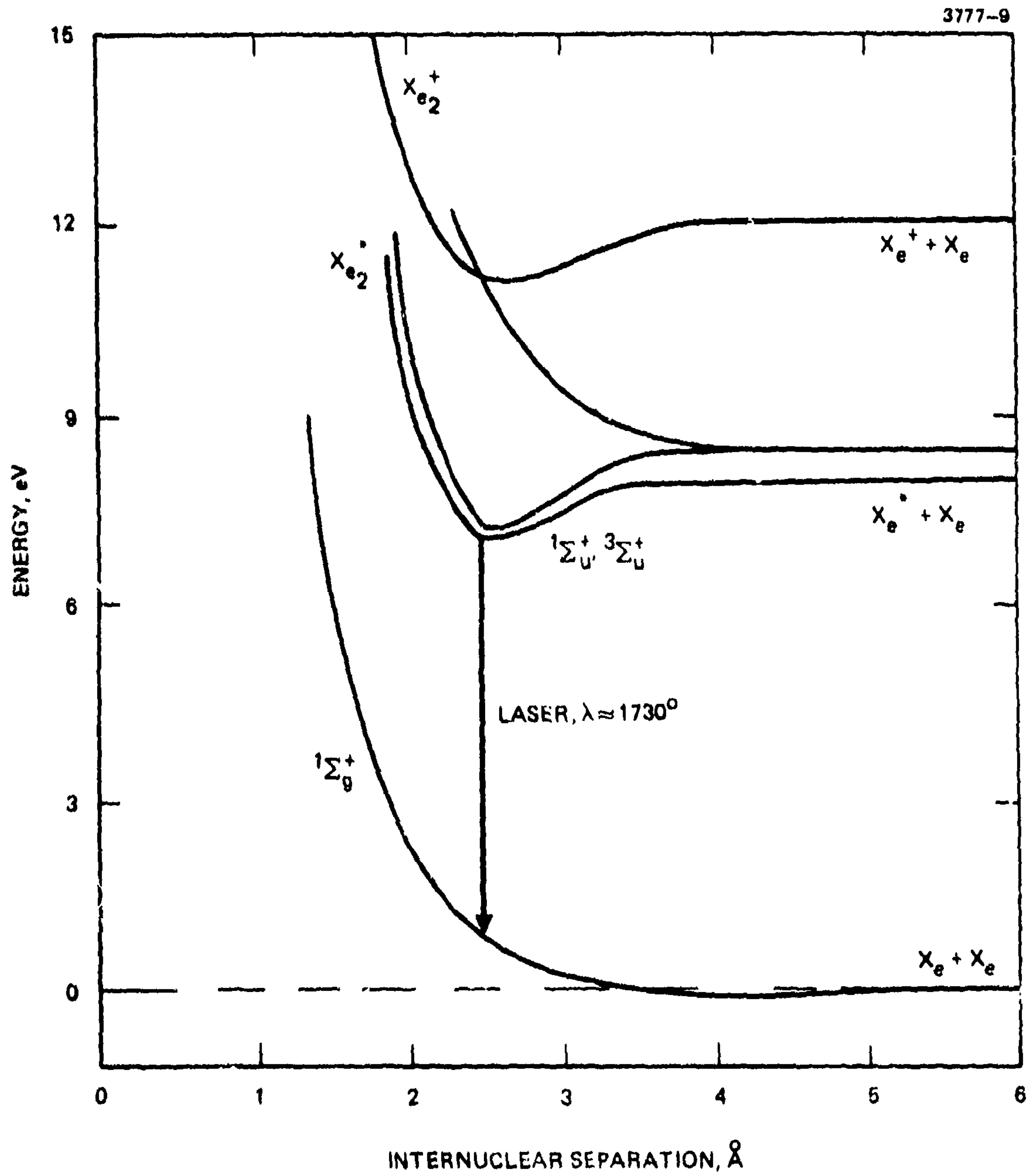

Fig. 6. Energy levels in the Xe_2 molecule,

$$Xe + e \rightarrow Xe^{+} + 2e \tag{1}$$

$$Xe^{+} + 2Xe \rightarrow Xe_2^{+} + Xe \tag{2}$$

$$Xe_2^{+} + e \rightarrow Xe^{*} + Xe \tag{3}$$

$$Xe^{*} + 2Xe \rightarrow Xe_2^{*} + Xe. \tag{4}$$

Since processes (2) and (4) involve three-body collisions they are significant only at high pressures; this is the principal reason that laser action optimizes for pressures in the range 10 to 100 atm.

Typical experimental conditions and laser performance in the Xe_2 laser (using electron beam pumping) are: operating pressures in the range 10 to 100 atm, specific power depositions in the range $5x10^7$ to $5x10^8$ W/cm^3, pump pulses of 50 nsec width, specific laser power outputs in the range 10^7 to $4x10^7$ W/cm^3, with reported efficiencies as high as 10%.

Recent experiments[16] have indicated that the performance of the Xe_2 laser is improved considerably by the addition of argon to excitation region. It is felt that the reaction of prime importance in this case is

$$Ar_2^{*} + Xe \rightarrow Xe^{*} + 2Ar \quad . \tag{5}$$

The laser pumping then proceeds via reaction (4) given above. The possibility of using argon-xenon mixtures is especially promising for discharge pumping, since argon has a higher thermal conductivity than xenon, and will thus aid in transferring heat to the walls.

2. Argon-Nitrogen Transfer Laser

The laser transition at 3577 Å in the argon-nitrogen laser arises from the same nitrogen band system (second positive) as the conventional low pressure pulsed nitrogen laser. The difference between these two systems is that the latter is pumped by direct electron collisions, while the former is pumped primarily by excitation transfer from argon metastables. A partial energy level diagram of the N_2 molecule is given in Fig. 7. The laser transition at 3577 Å originates on the v' = 0 ($C^3\pi_u$) state of N_2 and terminates on the v" = 1 ($B^3\pi_g$) state. By comparison, the predominant output in the low pressure nitrogen laser is at 3371 Å (v' = 0 to v" = 0). Figure 7 also shows the approximate energy of the argon $^3P_{0,2}$ metastables. These species can transfer energy to either $N_2(C)$ or $N_2(B)$, but the former state is favored because its resonance is at lower-lying stable vibrational levels.

Typical operating conditions in the Ar-N_2 transfer laser (with electron beam pumping) are[17]: an operating pressure of 600 to 5000 Torr in a 5% N_2-Ar mixture, specific power depositions in the range 5×10^6 to 2×10^7 W/cm^3, pump pulses of 50 nsec duration, specific laser power outputs of 1×10^4 to 4×10^4 W/cm^3, and an efficiency of approximately 0.2%.

C. Thermal Considerations

One significant advantage of small bore discharges is their capability to achieve large power input per unit volume. It is thus worthwhile to consider the requirements on discharge

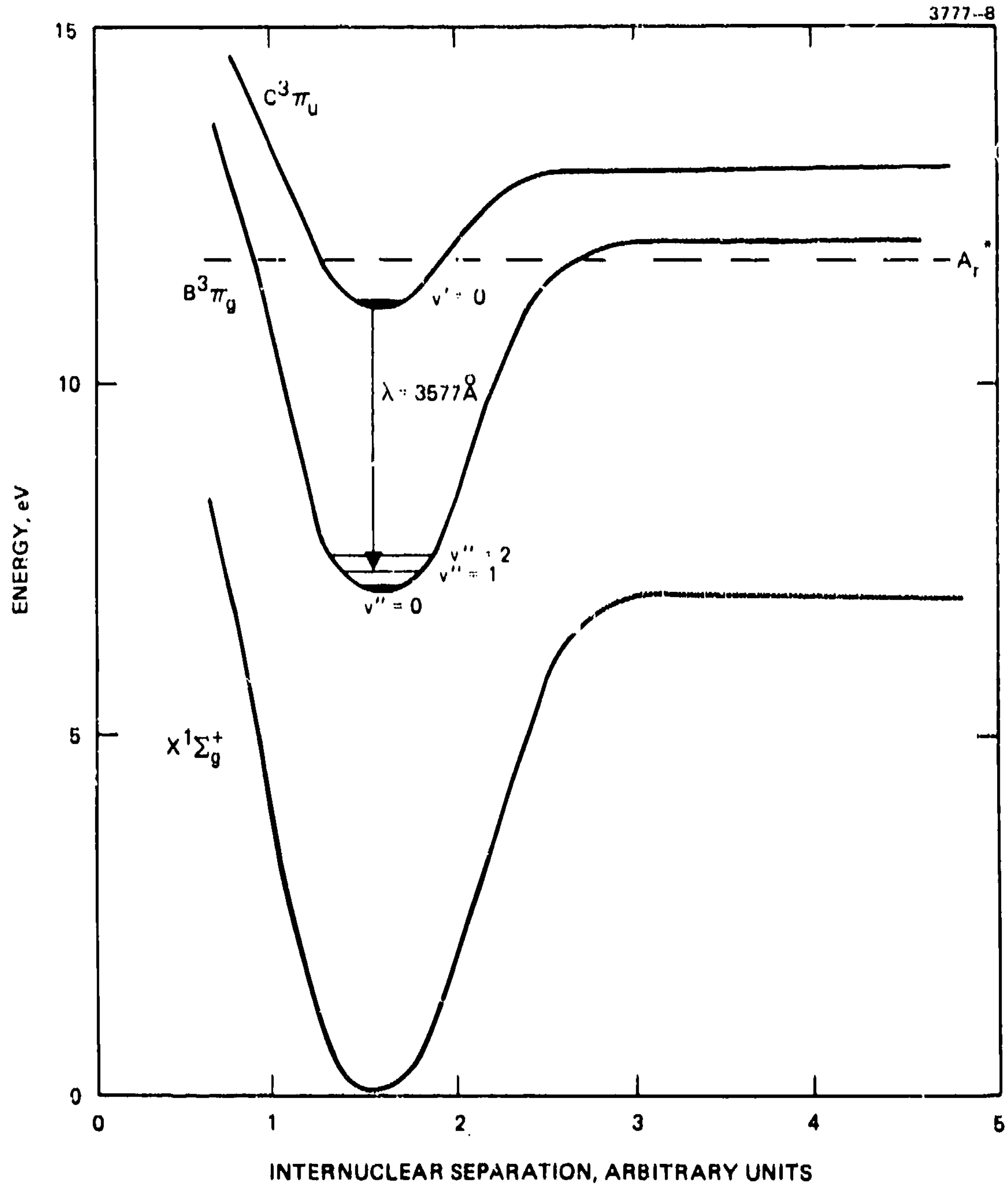

Fig. 7. Energy levels in N_2.

diameter for sustaining cw operation of a high pressure xenon discharge at large specific input powers. The variation of allowable power input with tube diameter is determined by two factors: heating of the gas within the discharge volume, and heating of the inner wall of the discharge vessel by conduction from the interior of the discharge. Considering gas heating first, we make use of the steady-state solution to the heat equation (in a cylinder of radius R) for a uniform heat source:

$$T(r) = T(R) + \frac{E}{4k}\,(R^2 - r^2), \tag{6}$$

where T(r) is the temperature at radius r, T(R) is the temperature at the outer boundary of the discharge, E is the input power per unit volume, and k is the thermal conductivity of the laser gas. On the axis of the discharge (r = 0),

$$\Delta T = T(o) - T(R) = \frac{ER^2}{4k} \quad . \tag{7}$$

Written in terms of power input per unit length (P), eq. (7) becomes

$$\Delta T = \frac{P}{4\pi k} \quad . \tag{8}$$

Thus if we are given a maximum allowable temperature difference ΔT, the allowable power input per unit volume varies inversely with the square of the radius, while the allowable input per unit length remains invariant.

We now consider the scaling of thermal loading on the walls of the discharge vessel. The steady-state solution of the heat equation for conduction through a cylindrical shell is given by

$$\Delta T_1 = T(R)-T(R_1) \approx \frac{R^2 \ln\left(\frac{R_1}{R}\right)}{2k} E, \tag{9}$$

where T(R) is the temperature of the inner wall (radius R), $T(R_1)$ is the temperature of the outer wall (radius R_1), k is the thermal conductivity of the wall material, and E is the discharge power input per unit volume. Writing (9) in terms of power input per unit length we obtain

$$\Delta T_1 = \frac{\ln\left(\frac{R_1}{R}\right)}{2\pi k} P. \tag{10}$$

As before, the allowable specific power input varies with the inverse square of the radius, while the allowable linear power input is invariant (assuming the ratio R_1/R does not change significantly).

In order to better visualize the scaling of power input in small bore discharges, we have plotted temperature difference as a function of discharge specific energy input (eqs. (7) and (9)) for the example of xenon gas in a quartz discharge tube of 5 mm outer diameter. The results are plotted for three different values of bore diameter in Fig. 8. Using these plots we are able to determine the maximum allowable input power density for specific values of gas and wall temperature difference. For example, we consider the case $\Delta T = \Delta T_1 = 1000^oK$, corresponding to an axial gas temperature of $\simeq 2300^oK$ (with water cooling of the outer walls). From Fig. 8 we see that in a 100 μm bore tube gas heating limits the power density to 2.5×10^4 W/cm^3, while wall heating limits the power density to 4×10^5 W/cm^3. These values are expected to be accurate to within approximately a factor of two, since the

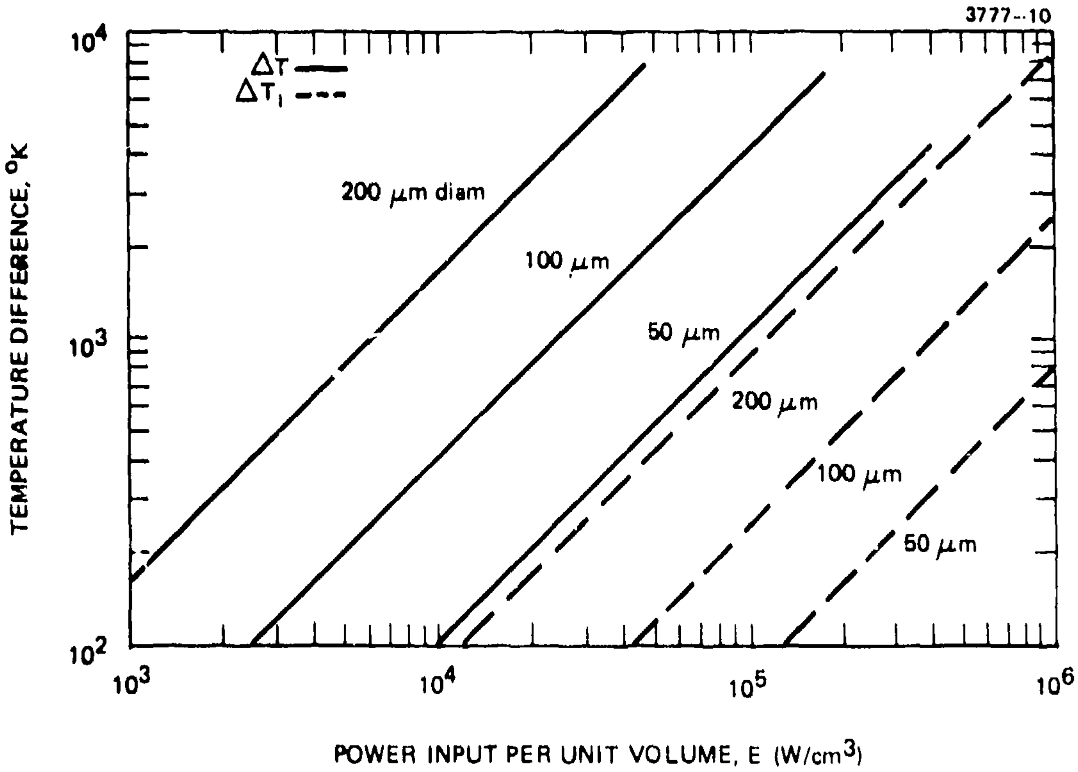

Fig. 8. Temperature difference versus specific power input.

thermal conductivity was assumed to be constant with temperature in plotting Fig. 8.

It is clear from the above example that gas heating is a more important factor than wall heating in limiting the permissible input power to the discharge. This is because xenon has the lowest thermal conductivity of all the rare gases. It should also be noted that the power limitation due to wall heating can also be relaxed if a wall material of higher thermal conductivity (such as BeO ceramic) could be used. However, BeO is not available with sub-millimeter drilled holes of sufficient length.

At this point it is desirable to estimate the pump power density required for threshold in the xenon excimer system. We start by writing an expression for the laser gain coefficient:

$$g \simeq \frac{\lambda^2 N}{8\pi\Delta\nu\tau} \quad , \tag{11}$$

where N is the inversion density, $\Delta\nu$ is the linewidth, and τ is the lifetime of the upper laser level. The pumping rate R is given by $R = N/\tau$, so that the required pumping rate for a gain g is

$$R = \frac{8\pi g\Delta\nu}{\lambda^2} \quad . \tag{12}$$

Assuming an efficiency η, the required discharge pump power is

$$E = \frac{8\pi h\nu g\Delta\nu}{\lambda^2 R} \tag{13}$$

for $h\nu \simeq 10$ eV, $g = 1\%/\text{cm}$, $\Delta\nu = 1.6\times10^{14}$ Hz, $\lambda = 1730$ Å and $\eta = 0.5\%$, we find $E = 4.2\times10^{7}\ \text{W/cm}^3$. This value of pump density is of the same order of magnitude as published values using e-beam pumping.

It is clear from Fig. 8 that the calculated threshold pump density cannot be sustained in a cw xenon discharge in a quartz capillary. This is true for even the smallest bore diameter considered (50 μm), although, in fact, precision bore quartz tubing of this size is difficult to obtain commercially. Rather than experiment with other bore materials and gas mixtures, it was decided to proceed with the xenon experiments using pulsed discharges. These can always be run with sufficient pulse duration to simulate cw operation, while keeping the duty cycle low enough to operate at reduced thermal loading.

D. Experimental Results

Most of our experiments on high pressure xenon and $Ar\text{-}N_2$ discharges were performed using a Pyrex discharge tube, shown in Fig. 9. The discharge capillary consisted of 100 μm precision bore Pyrex tubing divided into two discharge segments of 2.5 cm length. The electrodes are 0.050 in. tungsten pins, and an outer gas return path was provided to equalize any pressure difference built up during operation, and provide rapid pumping and filling of the rear segment of the tube. The glass diameter and wall thickness throughout the tube were kept at values which allowed the safe operation at pressures as high as 200 psi. The open end of the discharge tube is attached to a hollow brass flange which allows easy interchangeability of components. and which also incorporates a radial connection to the vacuum system and gas bottles. The laser tube-flange assembly is bolted to a large hollow flange which in turn could be bolted directly to the entrance slit body of a McPherson one meter normal incidence

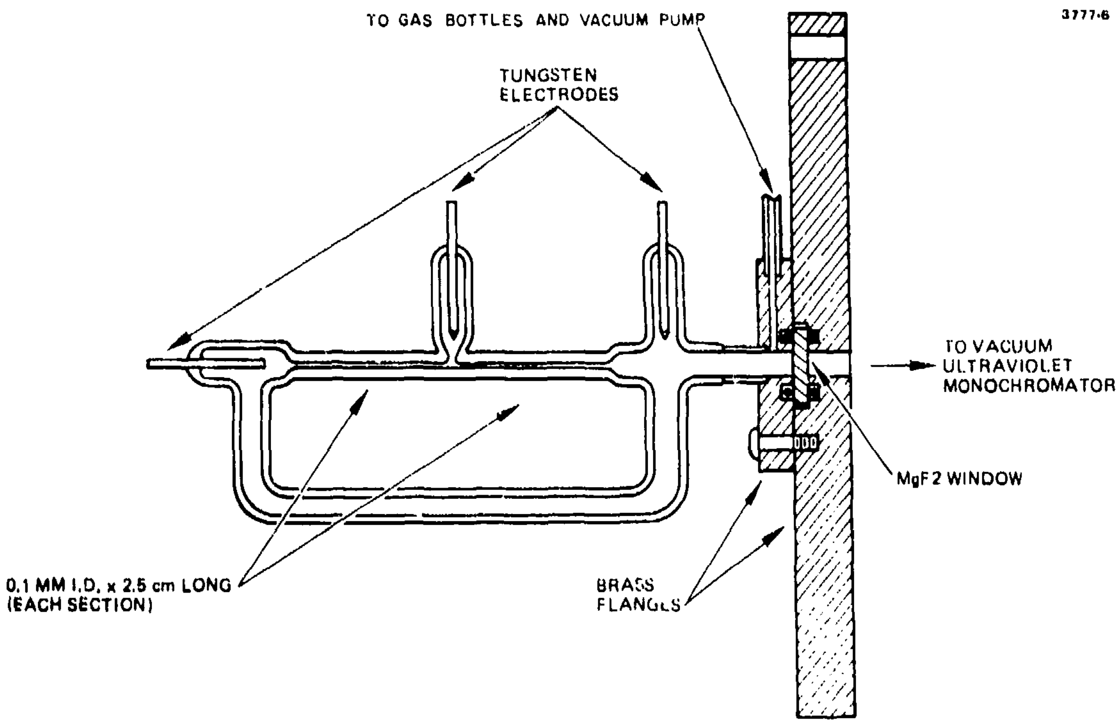

Fig. 9. High pressure experimental discharge tube.

vacuum ultraviolet monochromator. The two mated flanges also provide a mount for a MgF_2 window. This window transmits radiation at wavelengths down to approximately 1200 Å, and allows pumping of the monochromator to high vacuum, while maintaining high pressure in the discharge tube. The purpose of the two discharge segments is to allow endlight spectral observations over two different discharge lengths.

The discharge circuitry for this tube is shown in Fig. 10. The storage capacitor C is charged to 5 to 15 kV and then switched across the discharge tube when the thyratron fires. In order to aid in producing reliable breakdown of the discharge, a high voltage rf pulse is applied to a trigger wire wrapped around the tube at the same time as high voltage is applied to the electrodes. Two sizes of storage capacitor (260 and 780 pF) were used so that the variation of discharge characteristics with pulse duration could be studied.

With the discharge circuitry described above, we were able to generate stable, repetitive discharge pulses in xenon gas at the highest pressures ($\simeq$ 150 psi) investigated. Typical pulse durations were 200 to 800 nsec. In the 5% N_2-Ar mixtures, discharge triggering was reliable below 1 atm and was somewhat irregular at higher pressures. In all cases the pulse repetition rate was 10 Hz, with single shot operation as an option.

Our first experiments in the high pressure xenon system were concerned with measuring specific power deposition into the discharge volume. The discharge was operated over one of the two segments, and the time variation of the discharge voltage and current was recorded. Typical results at a pressure of

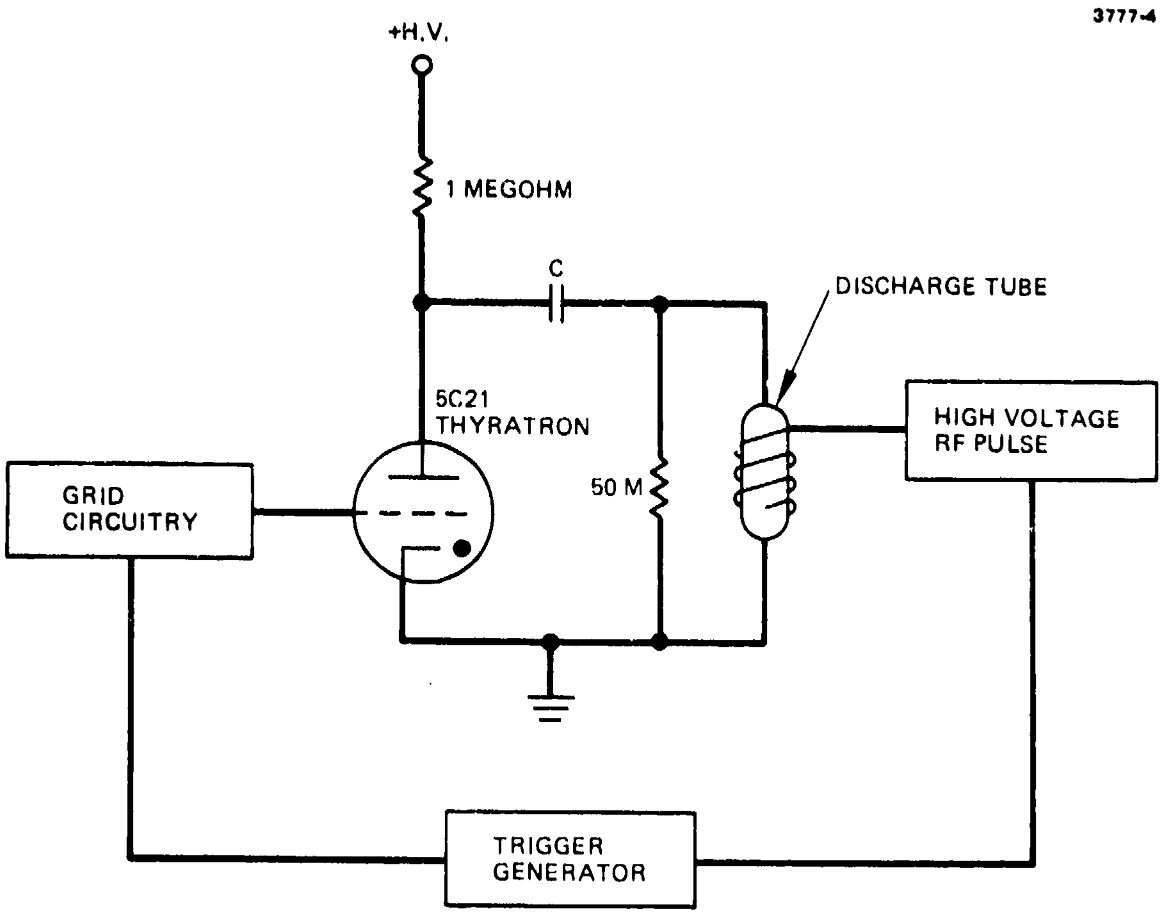

Fig. 10. Discharge circuit.

100 psig are plotted in Fig. 11. The specific power input, obtained by multiplying current and voltage, and then dividing by the capillary volume, is also shown. For this calculation we have assumed a uniform pumping distribution, and negligible power dissipation outside the capillary region. For the example given here, we see that a maximum specific power input of approximately 2×10^8 W/cm^3 was attained. At higher currents and voltages, power depositions as high as 4×10^8 W/cm^3 were attained at 100 psig, with slightly higher values at lower pressures. Comparing these values to the results of earlier threshold calculations, we see that we are able to deposit sufficient power into high pressure xenon to reach the calculated laser threshold. We have performed similar measurements in the Ar-N_2 system, where we again find that the available pumping should be sufficient for laser threshold.

The calculation of specific power deposition given above assumes a power input which is uniform across the discharge bore. This is an important experimental requirement, since a non-uniform or constricted discharge could cause large local heating and thus significant thermal dissociation of the desired molecular states. Local heating could also act to degrade medium homogeneity within the bore.

In order to examine the spatial variation of power deposition in the xenon discharge, we have photographed the bore region from the side using a microscope with a polaroid film back. The magnification was ≃ 50X. The photographs were obtained by opening

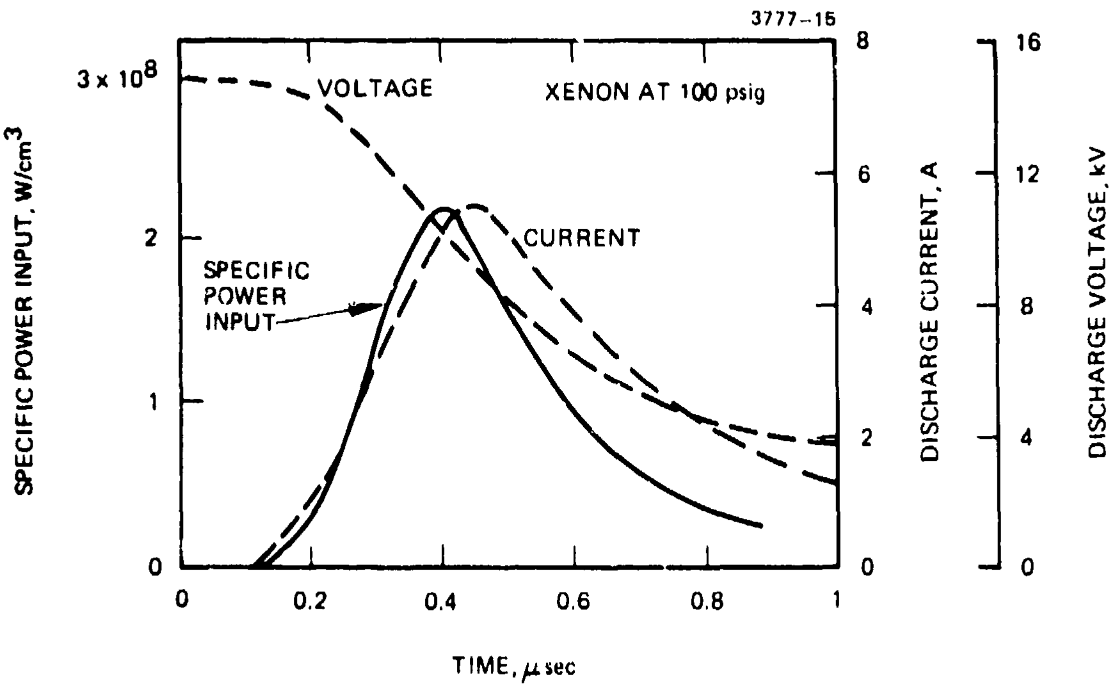

Fig. 11. Voltage, current, and specific power input versus time.

the shutter, initiating a single discharge pulse, and then closing the shutter. Typical photographs for two values of peak current at 80 psig pressure are shown in Fig. 12. We see definite evidence of constriction at the lower current while the bore at the higher current appears much more uniform. Since our photographs are time-averaged, it is possible that a uniform film exposure could result from a constricted discharge in rapid transverse motion. However, this explanation seems unlikely, since repeated pulses produce similar photographs at both current levels. In general our photographic studies of xenon discharges showed that constriction increased at higher pressures, and decreased at high currents. Most significantly we observe uniform discharges in the high-pressure high-current regime where laser threshold is expected.

We have also studied the emission spectra of xenon and Ar-N_2 discharges at the laser wavelengths. As the monochromator is scanned, the time-varying intensity is detected with a VUV sensitive photomultiplier. The output from the photomultiplier is then fed to a boxcar integrator, which averages the signal at its peak. The output from the boxcar is then fed to a chart recorder, which produces a time averaged spectrum as the monochromator is scanned.

A typical spectral scan near 1730 Å in xenon at 50 psig is shown in Fig. 13. The Xe_2 excimer band is clearly visible, and has a linewidth (160 Å) which agrees well with other spontaneous emission measurements.[14] The particular scan shown here was obtained from a discharge through one segment of the capillary; the linewidth for a discharge through both segments was found to be identical. This invariance of linewidth with discharge length

a

b

Fig. 12. 30 psig xenon discharge.
a. 5 A peak current.
b. 10 A peak current.

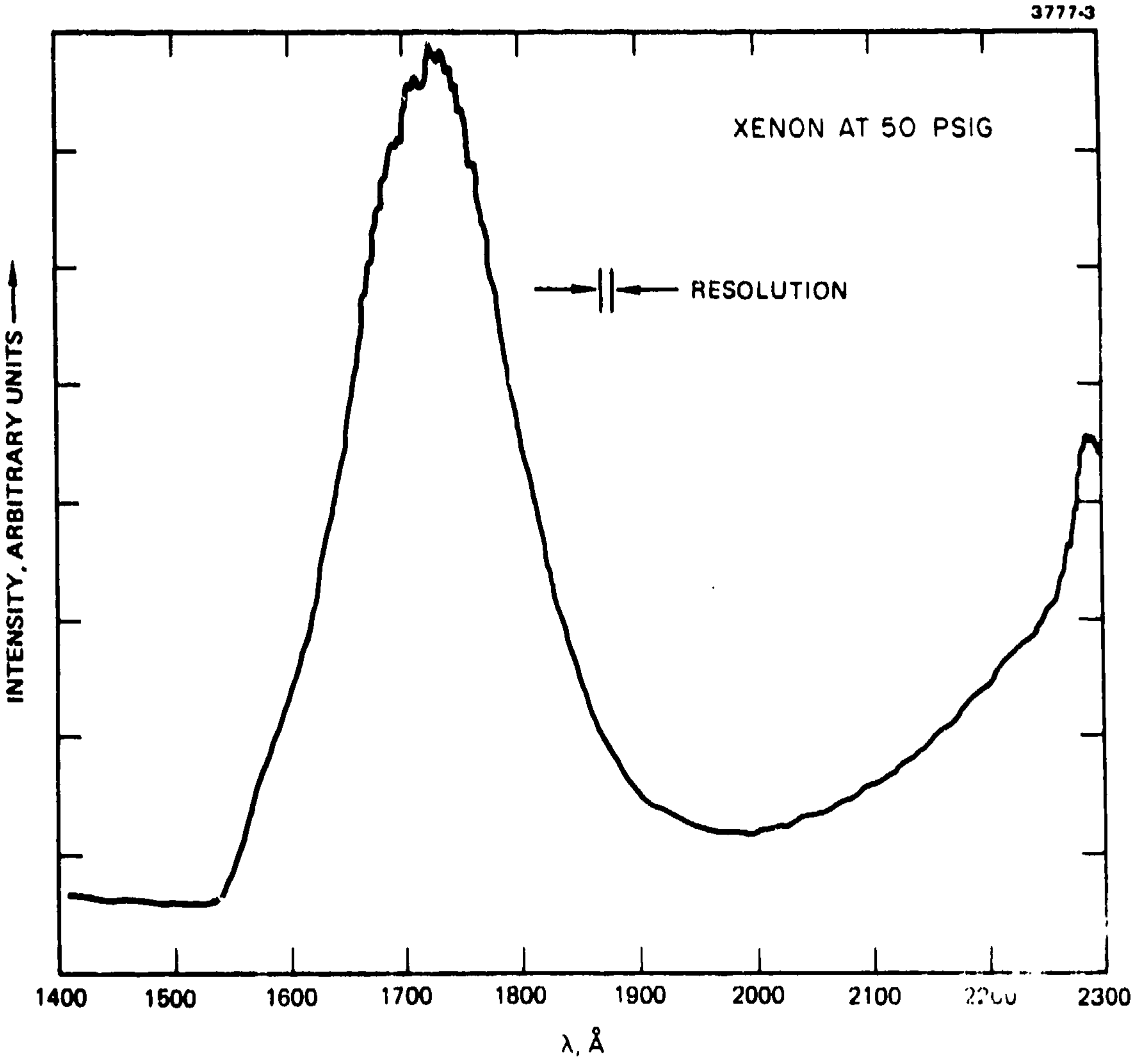

Fig. 13. Spectral output near 1730 Å from xenon discharge at 50 psig.

was observed at all pressures investigated, and indicates that if there is gain present in the discharge, it is not sufficient to cause any narrowing of the excimer band.

One feature which was common to all xenon spectra obtained was the significant intensity of a second band near 2300 Å; other stronger bands are also observed at longer wavelengths. These bands are not characteristic of spectra obtained from electron beam pumped xenon, and are thought to result from impurities of unknown origin. The xenon laser is particularly susceptible to impurities, since impurity molecules can easily absorb energy by collision with excited species in xenon which contribute to laser pumping. Although high purity xenon was used, our tube design and pumping system were not intended for ultraclean applications, and little could be done to reduce impurity levels.

In Fig. 14 we show a typical spectral scan from a discharge in a 10% N_2-Ar mixture at 3800 Torr, as well as from a discharge in pure nitrogen at 50 Torr. These spectra show the three lines (at 3371, 3577, and 3805 Å) which originate on the v' = 0 ($C^3\pi_u$) state and terminate on the v" = 0,1,2 ($B^3\pi_g$) state of N_2. The lines at shorter wavelengths in each case are not identified. We observe a background continuum in the high pressure Ar-N_2 mixture, which is thought to result from impurities.

E. Metal-Ceramic Laser Tube

The discharge tube used in the experiments reported earlier was very versatile and economical, but it suffered from two shortcomings. First, it did not contain provision for laser

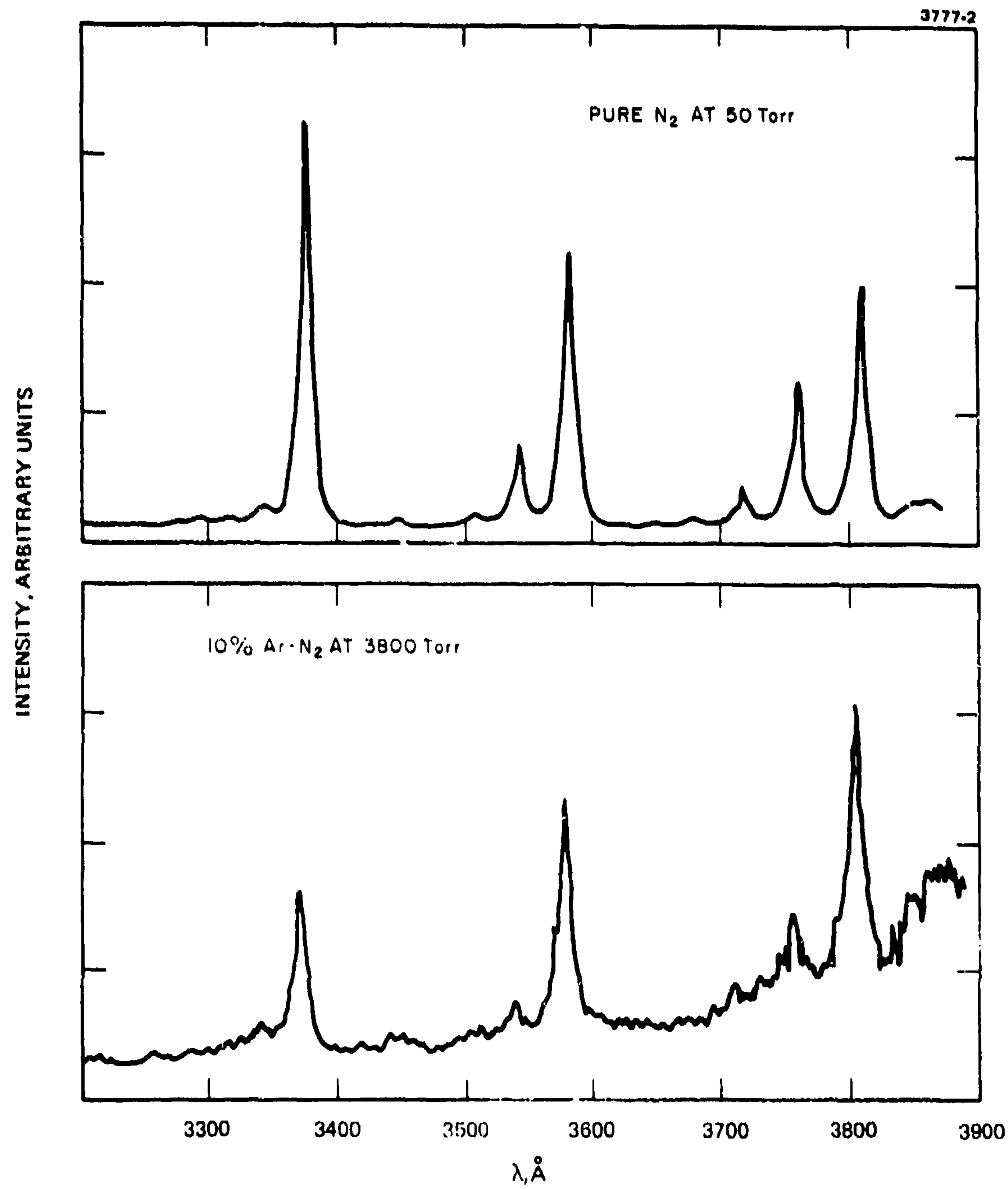

Fig. 14. Spectral output near 3500 Å from nitrogen discharge at 50 Torr (upper) and 10% N_2-Ar discharge at 3800 Torr (lower).

mirrors, so that no test for laser action could be made. Second, it was not intended for use in a low impurity vacuum system, so that tube cleanliness could not be ensured. Finally, the use of glass for containing the high pressures is dangerous, and limits the pressure range of operation. We thus decided to design a completely new tube in an attempt to overcome these problems. A cross-sectional view of the design is shown in Fig. 15. The important features of the tube are as follows:

1. In order to ensure improved pressure integrity, the outer walls are constructed entirely of metal and ceramic materials, except for the end windows which are of thick (ultraviolet quality) quartz.
2. The laser bore is formed by a quartz (or pyrex) capillary insert which can be replaced easily. Its length is approximately 7 cm.
3. The laser mirrors (of 2 in. radius of curvature) are internal to the pressure vessel to maintain low cavity losses, and are readily adjustable.
4. The mirror and bellows assemblies at each end are separately removable for ease in construction and cleaning.
5. A waveguide resonator is used, with mirror position adjusted so that the separation between the mirror surface and the end of the bore insert is equal to the mirror radius of curvature. This position provides low coupling loss into the waveguide at all wavelengths of interest.

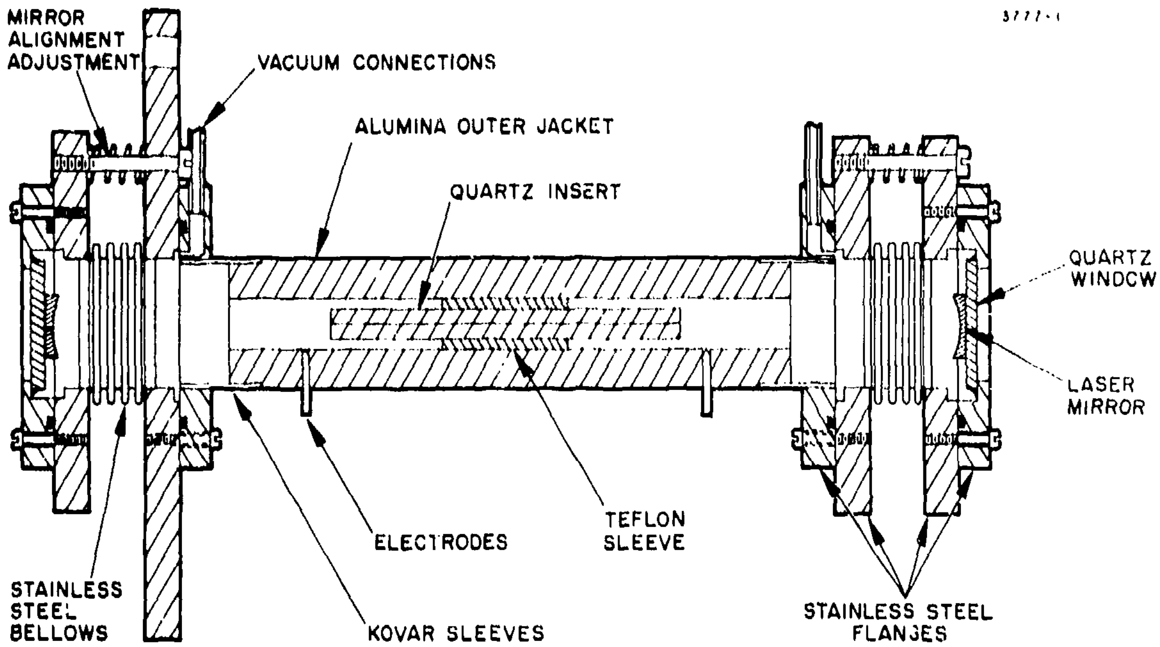

Fig. 15. Cross section of high pressure laser tube.

6. Except for the end flanges containing the laser mirrors, all components of the discharge tube are bakeable to high temperature in order to provide maximum cleanliness.
7. The large flange at one end is designed to bolt directly onto the entrance slit body of the vacuum ultraviolet monochromator.
8. The Teflon sleeve is mounted tightly to provide a solid mechanical mount for the bore insert, and to prevent discharge breakdown along its surfaces. Since there is no vacuum connection between the two ends of the vessel, separate tabulation is provided at each end for pumping and filling.

A photograph of the completed discharge tube is shown in Fig. 16, and a schematic of the vacuum and gas filling system is given in Fig. 17. Since the two ends of the discharge tube can not be electrically connected, a glass section was used for vacuum connection, although a ceramic section would serve equally well and provide better pressure integrity.

Since the search for laser action in a new system requires confidence in mirror alignment, we decided to optimize mirror alignment by first operating on the 4880 Å transition in ionized argon. For these initial experiments, a quartz insert with a 0.5 mm bore was used. However, in setting up to operate at low pressures (optimum at 4880 Å is $\simeq$ 0.1 Torr) unexpected outgassing problems and virtual leaks were discovered. Furthermore, the low

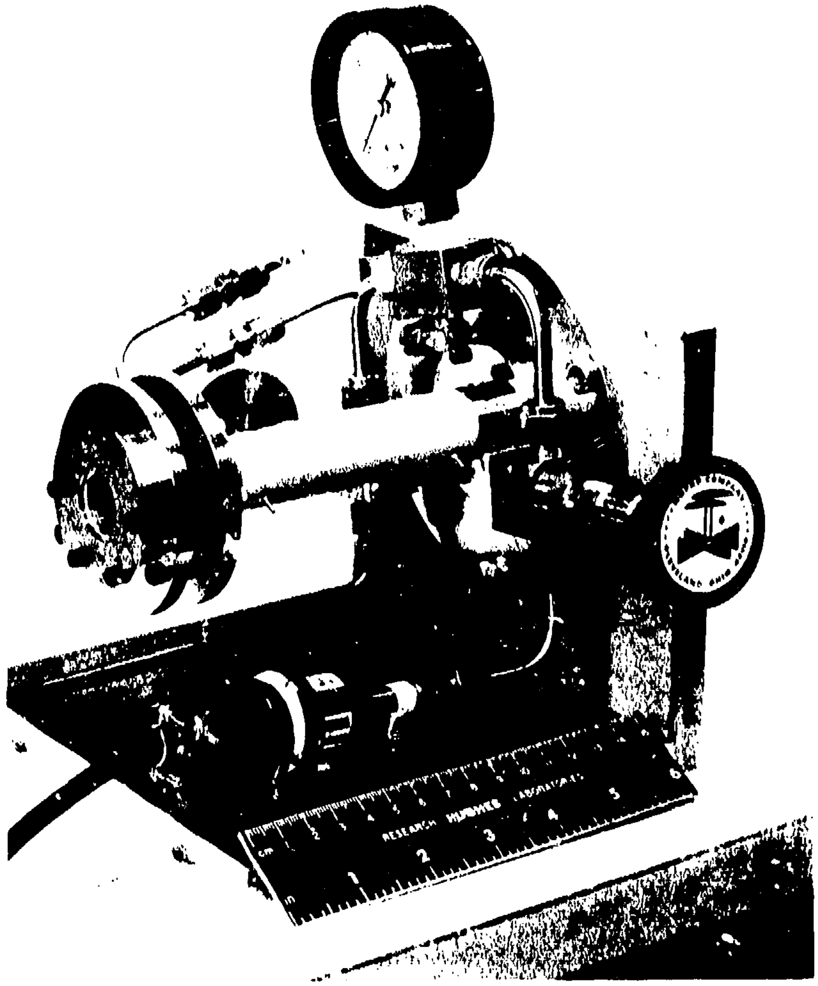

Fig. 16. Completed laser tube.

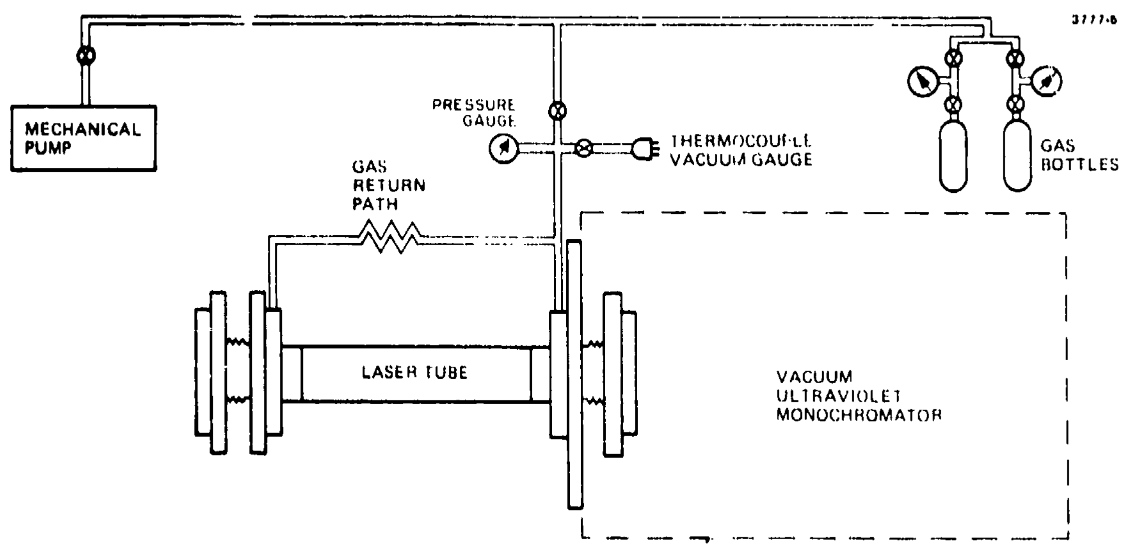

Fig. 17. Vacuum and gas fill system.

breakdown voltages encountered in low pressure argon required several adjustments of the gas return path and Teflon sleeves to ensure reliable discharging within the laser bore. These problems plus the late delivery of the tube prevented the adequate study of high pressure laser action before the expiration date of this contract. We were able to obtain laser oscillation at 4880 Å, but this was itself sporadic and not well optimized.

None of the problems described above are fundamental in nature, and we feel that continued studies of the Xe_2 and Ar-N_2 systems in our refined discharge tube carry a good chance of success, especially in the Ar-N_2 system (with lower pressure and pump threshold).

REFERENCES

1. P. W. Smith, Appl. Phys. Lett. 19, 132 (1971).
2. T. J. Bridges, E. G. Burkhardt and P. W. Smith, Appl. Phys. Lett. 20, 403 (1972).
3. R. L. Abrams, Appl. Phys. Lett. 25, 304 (1974).
4. C. K. Asawa, Appl. Phys. Lett. 24, 121 (1974).
5. P. W. Smith and P. J. Maloney, Appl. Phys. Lett. 22, 667 (1973).
6. S. K. Searles, VIII International Quantum Electronics Conference, San Francisco, Calif., June 1974, Abstract W.7.
7. G. Francis, Ionization Phenomena in Gases (Butterworth, London, 1960), Chapter 3.
8. E. I. Gordon and A. D. White, Appl. Phys. Lett. 3, 199 (1963).
9. R. L. Abrams and W. B. Bridges, IEEE J. Quantum Electron. QE-9, 940 (1973).
10. J. J. Hinchen, J. Appl. Phys. 45, 1818 (1974).
11. S. R. Byron, L. Y. Nelson and G. J. Mullaney, Appl. Phys. Lett. 23, 565 (1973).
12. L. Y. Nelson, S. R. Byron and G. J. Mullaney, 26th Gaseous Electronics Conference, Madison, Wisconsin, Oct. 1973, Abstract EB-1.
13. P. W. Smith, C. R. Adams, P. J. Maloney and O. R. Wood, VIII International Quantum Electronics Conference, San Francisco, June, 1974, Abstract W.9.
14. H. A. Koehler, L. J. Ferderber, D. L. Redhead and P. J. Ebert, Appl. Phys. Lett. 21, 198 (1972).

Preceding page blank

15. D. J. Bradley, M. Hutchinson and H. Koester, Optics Comm. 7, 187 (1973).

16. P. Hoff, J. Swingle and C. K. Rhodes, Optics Comm. 8, 128 (1973).

17. S. K. Searles, Appl. Phys. Lett. (to be published).